Mater. Res. Soc. Symp. Proc. Vol. 1145 © 2009 Materials Research Society 1145-MM04-12

Raman Spectroscopy of Group IV Nanostructured Semiconductors: Influence of Size and Temperature

A. Torres[1], O. Martínez[1], C. Prieto[1], J. Jiménez[1], A. Rodríguez[2], J. Sangrador[2], T. Rodríguez[2]
[1]GdS Optronlab, Edificio I+D, Universidad de Valladolid, Paseo de Belén, 1, 47011 Valladolid, Spain
[2]Departamento de Tecnología Electrónica, E.T.S.I. de Telecomunicación, Universidad Politécnica de Madrid, 28040 Madrid, Spain.

ABSTRACT

Group IV nanostructures have attracted a great deal of attention because of their potential applications in optoelectronics and nanodevices. Raman spectroscopy has been extensively used to characterize nanostructures since it provides non destructive information about their size, by the adequate modeling of the phonon confinement effect. However, the Raman spectrum is also sensitive to other factors, as stress and temperature, which can mix with the size effects borrowing the interpretation of the Raman spectrum. We present herein an analysis of the Raman spectra obtained for Si nanowires; the influence of the excitation conditions and the heat dissipation media are discussed in order to optimize the experimental conditions for reliable spectra acquisition and interpretation.

INTRODUCTION

The potential applications of nanoscaled semiconductor structures have raised a great deal of characterization effort. In particular, nanosized structures of group IV semiconductors have been the object of many studies. The properties of those nanostructures depend on their nanostructure and dimension; therefore, a great effort is paid to investigate simple ways to determine their dimension. Raman spectroscopy is a very powerful non destructive tool suitable to such study, because of the spectral changes related to the phonon confinement in reduced size structures [1-8]. The study of the lineshape of the first order phonon lines of the Raman spectrum may supply valuable information about the nanostructure size. The Raman spectrum is also sensitive to temperature and stress [9]; therefore, the Raman study can provide information about the thermal properties, such as the thermal expansion and the anharmonicity, which are crucial to model the heat dissipation and the thermal induced stresses, which are critical issues to design devices with optimal mechanical and heat transport properties.

As a consequence of the break down of the translational symmetry for reduced dimensions, the phonon correlation length becomes finite and the momentum selection rule is relaxed allowing scattering by phonons out of the zone center [1, 2]. The result of this is a softening and asymmetric broadening of the phonon modes. However, other factors induce similar changes in the Raman spectrum, which might mask the assessment of the nanostructure features. The phonon confinement effect can also occur in the presence of extended defects that breakdown the translational symmetry; in other words, the Raman spectra of structures with defects can induce erroneous estimations of sizes. Moreover, temperature plays a relevant role shaping the Raman spectrum, which needs to be considered if one looks for a straightforward interpretation of the Raman data. Usually, nanostructures are embedded in an environment medium, which can induce mismatch stresses, because of the different lattice parameters, or

different thermal expansions. Furthermore, the surrounding media can have poor thermal conductivity, as it is the case of nanowires (NWs) in air. The poor heat dissipation of these systems can artificially change the Raman spectrum because of the laser induced overheating during the spectra acquisition, which is truly critical for NWs [7, 11].

We present herein an analysis of the influence of laser induced temperature enhancement in the Raman spectra of Si NWs, using a phonon confinement model. The Raman parameters are described in terms of the combined effect of temperature and size. These data are compared with the experimental results obtained on Si NWs under different excitation power densities; measurements were carried out with the NWs in air and submerged in deionized water to enhance the thermal conductivity of the surrounding environment. A discussion of the main issues regarding the Raman spectra of Si NWs is presented.

EXPERIMENTAL DETAILS

The Si NWs were fabricated by Low Pressure Chemical Vapour Deposition (LPCVD) on (100) Si substrates using Si_2H_6 as precursor gas. The Si substrates were dipped in HF, rinsed for 30 s in APTES, dried with N_2 and subsequently rinsed in a colloidal suspension of Au particles 30 nm in diameter for 180 s. The samples were immediately loaded into the LPCVD reactor, where they were annealed at 500 ºC for 60 min. The subsequent NW growth process was carried out also at 500 ºC for 30 min and with a partial pressure of Si_2H_6 of 40 mTorr. Typical NWs had diameters ranging from 15 to 120 nm and several μm length depending on the growth conditions. The NWs were observed in the scanning electron microscope (SEM), Fig. 1. However, the crystalline core should be smaller, since usually a thick SiO_x shell is present.

The Raman spectra were acquired with a Labram UV-HR 800 Raman spectrometer from Jobin Yvon. The NWs were not detached from the substrate, they appear as seen in Fig. 1, forming tangles of wires. The measurements were done in air and with the NWs submerged in deionized water. The excitation was done with an Ar^+ laser (514.5 nm).

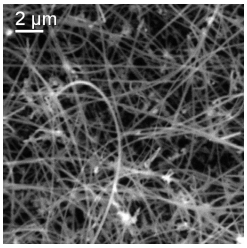

Figure 1. SEM image of Si NWs.

DISCUSSION

The Raman spectra of the NWs samples present a low frequency amorphous tail, arising from the deposit of amorphous Si on the substrate, and a crystalline component, which the shape and frequency deviates from the spectrum of the control silicon monocrystalline wafer. One observes that the phonon band asymmetrically broadens, and the peak frequency shifts to the low frequency, which is the typical signature of phonon confinement. The Raman spectra for different laser power densities, scaled by using neutral filters, are shown in Fig. 2a; in these

spectra the amorphous tail was subtracted. The first order phonon mode of Si shows downshift and broadening with increasing laser power excitation. The corresponding Raman spectra measured with the NWs submerged in water are shown in Fig. 2b, the control spectrum of bulk Si is also included. The two series of spectra evidence how the deformations of the phonon bands are dependent on the surrounding media and the laser power density. This behaviour suggests that the spectrum is contributed by the heating of the NWs when they were exposed to air; while thermal effects seem to be negligible in the case of the NWs submerged in water; which is due to the higher thermal conductivity of water (0.58 W/mK vs 0.024W/mK).

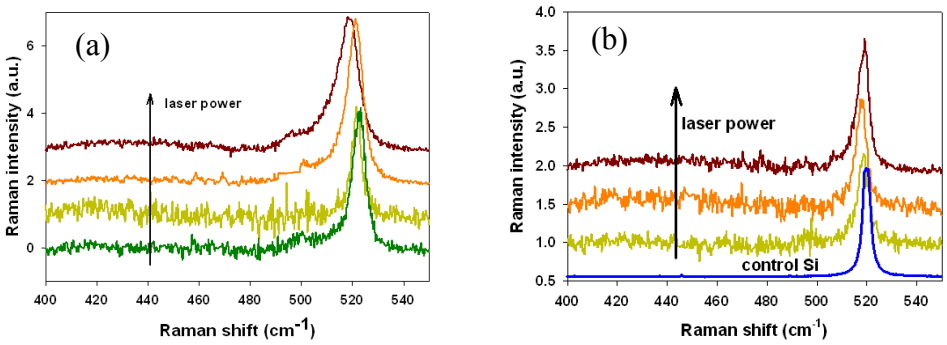

Figure 2. Raman spectra in air (a), and water (b). The laser power densities are 250 W.cm^{-2} (only in a), 750 W.cm^{-2}, 1.25 kW.cm^{-2}, and 2.5 kW.cm^{-2}. The control spectrum is also shown.

The Raman parameters of the spectra of Fig. 2 are represented as a function of the laser power density in Fig. 3. The power densities for the two experimental configurations, air and water, were normalized using a series of reference samples, in order to render the two series of measurements comparable. One observes that the low frequency half width, Γ_a, broadens with increasing excitation laser power. However, in the case of the spectra recorded in water there is not evolution of Γ_a with the excitation laser power, which means that the spectra recorded in water reveal the effect of the phonon confinement. One can extrapolate to excitation power zero and compare the Raman parameters to those of the control Si substrate, $\Delta\omega=0$, and $\Gamma_a = 1.4$ cm^{-1}. Note that even for the lowest excitation power density in the case of the spectra acquired in air, Fig. 2a, some heating effect is present; see that the two lines of Fig. 3, in air, and in water, respectively, intersect at very low laser power.

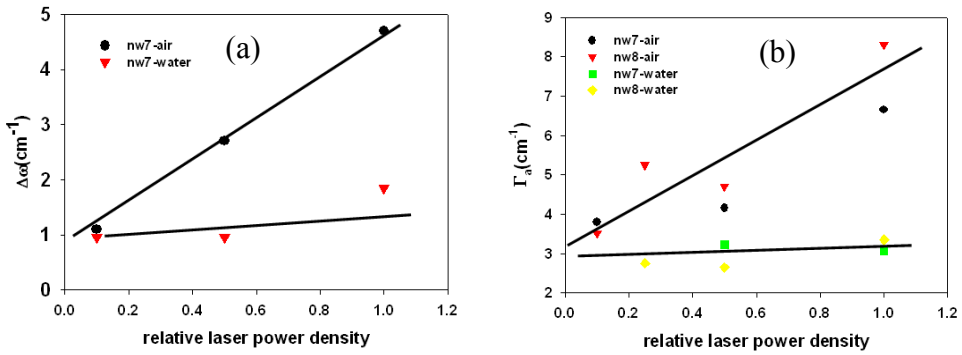

Figure 3. Raman parameters $\Delta\omega$ (a), and low frequency half width Γ_a (b), obtained by fitting the spectra corresponding to the two experimental configurations (air and water). The data corresponding to two samples (nw7 and nw8) are plotted.

The observation of the phonon confinement effects suggests that the crystalline core is much smaller than the diameter observed by SEM, because phonon confinement is not appreciable for dimensions above 20 nm. Therefore one can assume that either they have crystalline cores less than 15 nm in diameter, with a thick oxide surrounding shell, or they are twinned with the corresponding symmetry breakdown, contributing to the phonon confinement.

The average size of NWs can be determined using a phenomenological phonon confinement model [2, 7]. These models are based on the uncertainty of the phonon momentum, because of the reduced size of the structures. In reduced size structures phonons with $q \neq 0$ are allowed to contribute to the Raman spectrum. The phenomenological models use different localization functions. In order to determine the size of the crystalline cores of the NWs the Raman bands were fitted according to a modified correlation length model. Assuming a Gaussian localization factor [1, 2] the Raman intensity can be expressed as:

$$I(\omega, L) \propto \int \exp\left(-\frac{q^2 L^2}{16\pi}\right) \frac{d^3 q}{\left[\omega(q) - \omega_o\right]^2 + \left(\frac{\Gamma_o}{2}\right)^2} \tag{1}$$

where $\omega(q)$ is the phonon dispersion function, ω_o and Γ_o are the phonon frequency and the full width at half maximum (FWHM), respectively, of the bulk material; the linewidth includes the instrument broadening contribution, which in our experimental conditions gives a full width at half maximum for a high quality Si bulk crystal of 2.8 cm^{-1} at room temperature. $\omega(q)$ is the phonon dispersion relation, and the phonon wavevector modulus, q, is expressed in units of $2\pi/a$, where a is the lattice parameter of crystalline Si, and L is the diameter of the confinement volume expressed in units of the lattice parameter. At the present time we have not transmission electron microscopy (TEM) images of the NWs; however, we assume a cylindrical symmetry, with the diameter much smaller than the length, according to the external aspect of the wires, Fig. 1. The phonon dispersion relation for pure Si can be approximated by the following expression:

$$\omega(q, T) = [A(T) + B(T) \cos(\pi q/2)]^{1/2} \tag{2}$$

where A(T) and B(T) are determined from the phonon dispersion curve [12].

The Raman phonon bands depend on the temperature because of the thermal expansion and the anharmonicity of the vibrational potential energy [5, 7, 9, 10]. The dependence of the Raman spectrum with temperature for bulk material was previously obtained on the control Si wafer. The variation of ω_o and Γ_o with temperature were approached to a linear function:

$$\omega_o(T) = 521.9 - 0.0247 * T(^oC) \tag{3}$$
$$\Gamma_o(T) = 2.8 + 0.0102 * T(^oC)$$

The temperature coefficients of Eq. 3 for phonons with $q \neq 0$ are not available, therefore the full phonon branch was assumed to follow Eq. 3. Note that this is a first approximation, because one can expect a variation of the anharmonic constants of nanostructures respect to the anharmonic constants of the bulk material. To the best of our knowledge, no reliable data exist about the influence of the size on the anharmonicity and the thermal expansion of Si NWs.

Nevertheless, a dependence of the anharmonic coefficients with nanocrystal size was reported for CdSe nanocrystals embedded in germanate glass [13].

The calculated spectra are shown in Fig. 4; in Fig. 4a they are shown the spectra at room temperature for different NWs diameters, while in Fig. 4b they are shown the spectra at different temperatures for a diameter of 8 nm. Temperature shifts the peak to the low frequency, and broadens the band, which becomes more symmetric, respect to the confinement profile.

Fig. 5 summarizes the results of the modeling; peak frequency and Γ_a are represented as functions of the NW diameter for different temperatures, in Figs. 5a and 5b, respectively. The peak frequency shift related to phonon confinement is very small for cylindrical symmetry, in agreement with [7], while the bandwidth presents a significant broadening for diameters below 8 nm.

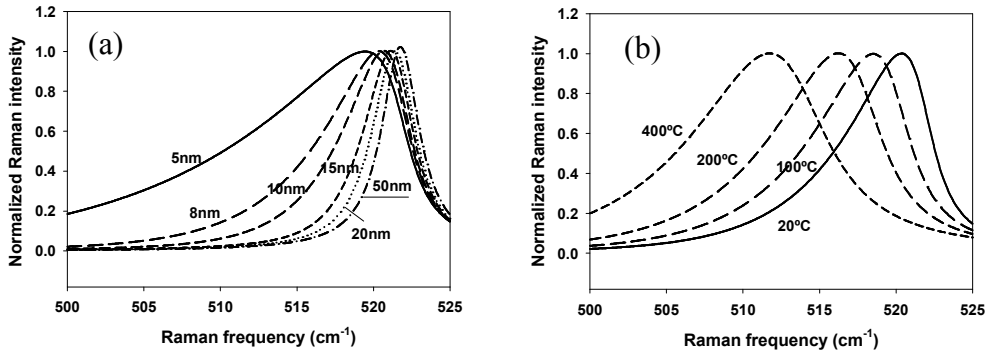

Figure 4. Calculated spectra (a) at 20 ºC for different NWs diameters, (b) for a diameter of 8 nm at different temperatures.

Concerning the temperature dependence of the Raman parameters, in large structures, one observes that for increasing temperatures the phonon bands are softened and broadened according to empirical relations close to those of bulk Si, which are very close to those corresponding to 30 nm diameter in Fig. 5. The bands for sizes below 8 nm remain strongly asymmetric even at high temperature. Therefore, the band shape for small NW diameters is mainly determined by the phonon confinement. Regarding the phonon peak frequency, the effect of temperature dominates over the phonon confinement, which is consistent with the very small peak shift calculated for the cylindrical symmetry.

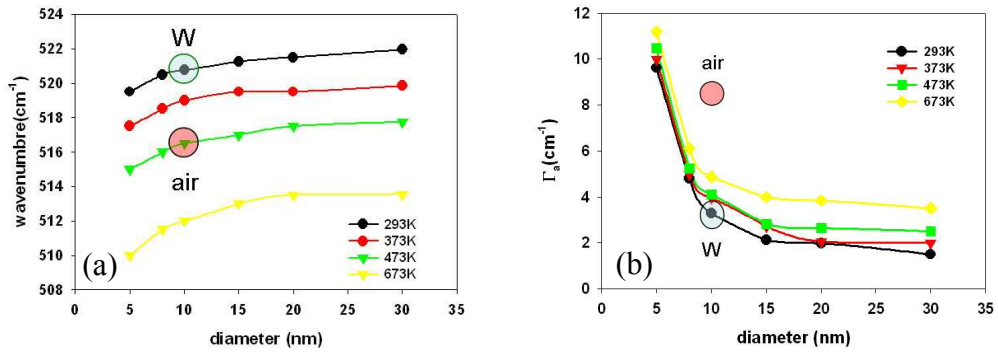

Figure 5. Calculated Raman parameters: phonon frequency (a) and Γ_a (b), as a function of NW diameter for different temperatures. The circles correspond to the experimental values obtained in water (W) and in air (laser power density 2.5 kWcm^{-2}).

The Raman parameters measured in water lay in the circle area labeled W in Fig. 5; according to those values one can estimate that the NWs have an average diameter around 10 nm. In air, the NWs are overheated by the laser beam, with red shifts as large as 5 cm^{-1}, and Γ_a of 8 cm^{-1} for the highest laser power density used, ≈ 2.5 $kW.cm^{-2}$; the crude analysis of these data would give NW diameters close to 5 nm, see Fig. 5. The in air data parameters lay in the circles labeled air, one observes that the peak frequency shift and the Γ_a values are not compatible in the frame of the model proposed. Therefore, the Raman spectra of the NWs in air are distorted by the laser induced heating, resulting in a temperature increase of several hundred ºC. Such temperature increase is not sufficient to fit the spectra obtained in air; therefore, further approaches should require the use of temperature gradients in order to account for the observed band profile.

CONCLUSIONS

The Raman spectrum of Si NWs is severely influenced by the excitation conditions and the environment media. Heating induced by the laser beam contributes in a critical way to the shape of the phonon band. Therefore, a careful analysis of the experimental conditions and the phonon band profiles is necessary to extract straightforward information of the Raman spectra of these structures.

ACKNOWLEDGMENTS

This work was funded by the Spanish Government (Grant: MAT-2007-66181) and by the Consejería de Educación de la Junta de Castilla y León, Project No. VA051A06 (GR202).

REFERENCES

1. H. Richter, Z.P. Wang, and L. Ley, Sol. St. Commun. **39**, 625 (1981).
2. I.H. Campbell, and P.M. Fauchet; Sol. St. Commun. **58**, 739 (1986).
3. J. Zi, K. Zhang, and X. Xie, Phys. Rev. B **55**, 9263 (1997).
4. B. Li, D. Yu, and S.L. Zhang, Phys. Rev. B **59**, 1645 (1999).
5. P. Mishra, and K.P. Jain, Phys. Rev. B **62**, 14790 (2000).
6. M.J. Konstantinovic, S. Bersier, X. Wang, M. Hayne, P. Lievens, R.E. Silverans, and V.V. Moshchalkov, Phys. Rev. B **66**, 161311(R) (2002).
7. S. Piscanec, M. Cantoro, A.C. Ferrari, J.A. Zapien, Y. Lifshitz, S.T. Lee, S. Hofman, and S. Robertson, Phys. Rev. B **68**, 241312 (R) (2003).
8. S. Bhattacharyya, and S. Saumi, Appl. Phys. Lett. **84**, 1564 (2004).
9. J. Jiménez, I. de Wolf, J.P. Landesman, in *Microprobe Characterization of Semiconductors*; vol.17 of Optoelectronic properties of semiconductors and superlattices, Vol 17, ed. by J. Jiménez (Taylor and Francis, New York 2002), ch.2.
10. J. Jiménez, A. Torres, E. Martín, and J. P. Landesman; Phys. Rev. B **58**, 10463 (1998).
11. H. Scheel, S. Reich, A.C. Ferrari, M. Cantoro, A. Colli, and C. Thomsen, Appl. Phys. Lett. **88**, 233114 (2006).
12. S. Wei, and M.Y. Chou, Phys. Rev. B **50**, 2221 (1994).
13. A. Tanaka, S. Onari, and T. Arai, Phys. Rev. B **45**, 6587 (1992).